Int J Heat Mass Transfer Vol 33 No 11, pp 2451-2462 1990
Printed in Great Britain

0017-9310 90 $3 00+0 00

A fundamental study of the heat transfer and flow situation around spacers (a single row of several cylindrical rods in cross flow)

K ICHIMIYA
Department of Mechanical System Engineering, Yamanashi University, Takeda-4, Kofu, Yamanashi 400, Japan

and

N AKINO and T. KUNUGI
Japan Atomic Energy Research Institute, Tokai-mura, Nakagun, Ibaragi 319-11, Japan

(*Received* 25 *August* 1989)

Abstract—This paper describes the characteristics of heat transfer and flow around several spacers (a single row of several cylindrical rods) in cross flow on a heated surface in a parallel plate duct Temperature distributions are obtained by using a thermosensitive liquid crystal film and a narrow band optical filter method that does not require human color perception Apparent local Nusselt numbers between two cylindrical rods are expressed as a function of Reynolds number, local position and pitch of the cylindrical rods The pitch and Reynolds number affect the wake flow patterns which are classified into three domains

INTRODUCTION

In order to examine the fundamental effects of spacers set in fuel elements of a multi-purpose high temperature gas cooled reactor, the effects of a cylindrical rod in a parallel plate duct on heat transfer were measured by using a liquid crystal sheet from a previous study [1] The present paper describes the characteristics of heat transfer and flow distribution around several cylindrical rods in cross flow

There have been some studies for local and mean heat transfer on the side surface of rods in a flow passage [2, 3] Heat transfer and flow characteristics around three circular cylinders on a smooth plate, relating to the compactness of heat exchangers, were experimentally obtained by changing the pitch of the cylinders [4]. For tube banks, the influence of the tube arrangement [5–7] and equipment size [8] on convective heat transfer and flow resistance were investigated experimentally. The rate of change of these characteristics were related to changes in the Reynolds number VanFossen [9] performed the experiment with short pin fins to increase the heat transfer to the coolant in the trailing edge of a turbine blade Heat transfer data for short pin fins were found to be lower than data for long pin fins and fell on a single correlation line. In many cases the average heat transfer in the test section and the local heat transfer on the circular rods have been examined experimentally. Two-dimensional temperature distributions and the local heat transfer between two circular rods on the wall of the flow passage are not as available in the literature

Liquid crystals have been used for indicating temperature change and have been applied for heat transfer research [1, 10, 11] Ireland and Jones [12] applied a thermochromic liquid crystal to measure the temperatures of the internal wall and a cylindrical rod itself in a duct. Hippensteele *et al* [13] recently obtained high-resolution heat transfer coefficients on a vane surface of a gas turbine by using a liquid crystal, heater-element composite sheet However, human color perception is included in these methods when the liquid crystal sheet is calibrated for color vs temperature.

The main purpose of the present study is to examine the effects of several rods as mentioned above, especially the apparent local heat transfer between two rods and the relationship between heat transfer and flow characteristics Especially, heated surface temperatures are measured by an improved liquid crystal thermometry, excluding human color perception, in which we developed a quantitative analysis of the color distribution of a liquid crystal sheet using the optical filter method by sharp-band-pass characteristics [14]

EXPERIMENTAL FACILITY AND PROCEDURE

Experimental facility

Figure 1 shows a schematic diagram of the experimental facility. The test section set on the suction side of a blower was composed of a parallel plate duct the length, width and height of which were 2100, 230 and 10 mm, respectively, and the bottom plate of which was insulated. Air was used as the working fluid The heating section contained a stainless steel foil heater the thickness and length of which were 0 05 and 750 mm, respectively, and which was set on the upper plate

NOMENCLATURE

- D diameter of circular rod
- D_H hydraulic diameter, $2H$
- H distance between upper and lower plate in a flow passage
- n index of y/D (equation (3))
- Nu Nusselt number, $\alpha \cdot 2H/\lambda$
- Pi pitch of rods
- q heat flux
- Re Reynolds number, $U_m \cdot D_H/\nu$
- T_b bulk temperature of fluid
- T_w heated surface temperature
- U_m average velocity across the cross-sectional area
- x longitudinal distance from the center of a rod
- y distance in width from the center of a rod

Greek symbols

- α local heat transfer coefficient
- λ thermal conductivity
- ν kinetic viscosity

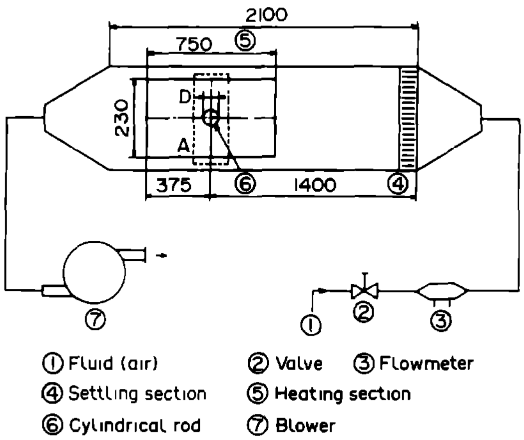

FIG. 1. Schematic diagram of the experimental facility.

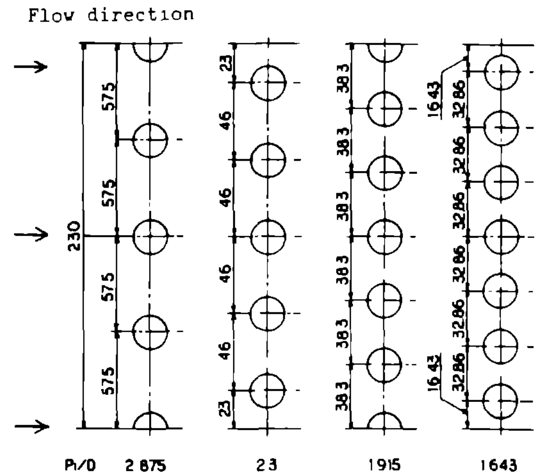

FIG. 2. Arrangement of circular rods.

at 1025 mm from the entrance. Electrical connections were made to a copper bus-bar soldered to the edge of the stainless steel foil. This allowed constant heat flux to be simulated by passing an alternating current (up to 2 V at 50 A) along the length of the stainless steel foil. Several circular rods (20 mm o.d.) were set at a position 375 mm from the starting point of heating. A circular rod was always put at the center of the width. Other rods were arranged normal to the flow direction and located symmetrically about the rod at the center of the width as shown in Fig. 2. Wall temperature measurements were made by using a cholesteric type liquid crystal sheet and pictures were taken of the color distribution by a CCD (charge coupled device) camera (refer to Fig. 3). Entrance and exit temperatures of the air were measured directly by thermocouples.

In order to relate the heat transfer to the fluid flow distribution, a flow visualization was performed by using a recirculating water bath with a parallel plate duct the width and length of which were 300 and 2000 mm, respectively. The size of the circular rod used in these studies was 14 mm high by 28 mm in diameter to make it similar to the heat transfer flow passage. Pearl pigment (mica particles) covered by oxidized titanium was used as the flow visualization medium.

Temperature measurement by liquid crystal sheet (optical filter method by sharp-band-pass characteristics)

Liquid crystal material can be adhered to or painted on a surface. Two-dimensional temperature distributions can be easily visualized as a color distribution. However, it is sometimes insufficient for quantitative measurement since human color perception must be used to evaluate temperature from color. We studied a method that is based on optical filters with sharp-band-pass characteristics to extract isochromatic regions corresponding to isothermal areas [14]. Figure 3 shows the cross section of the flow passage and a schematic diagram of the measurement system. The color changes of the chosen liquid crystal cover a temperature range from 27 to 39 C. The color patterns were observed by a CCD camera and the output from the camera was recorded by a video tape recorder. The color observations were carried out by changing narrow band optical filters mounted in front of the camera. The recorded images were transcribed on the monitor connected with an image processor (called IP-2) and the digitized images were transferred to a 16-bit digital computer and were recorded on floppy disks. The relationship between filter wave-

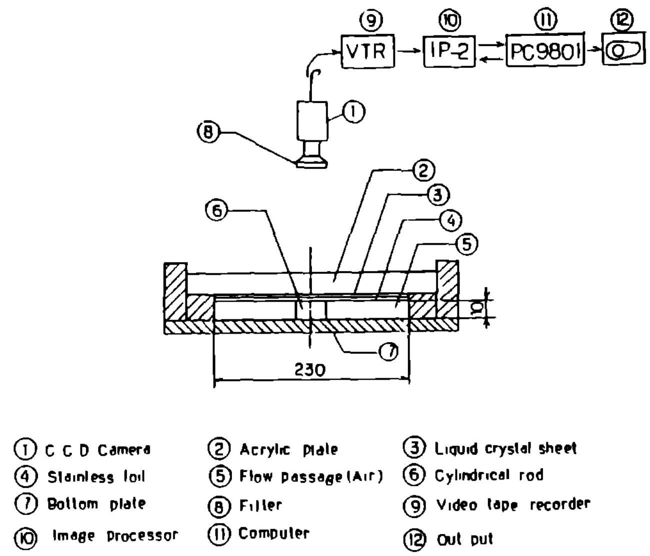

FIG 3 Schematic view of the test section

Table 1 Relationship between wavelength and temperature

Wavelength (nm)	Temperature (°C)
477.0	34.9±0.3
500.0	33.0±0.4
524.0	32.1±0.2
537.5	31.5±0.1
548.5	31.2±0.1
561.5	30.7±0.1
577.0	30.5±0.2
589.0	30.2±0.2
598.5	30.1±0.2
627.0	29.7±0.0
651.0	29.5±0.1
672.0	29.3±0.1
700.0	28.9±0.2
729.5	28.8±0.2
747.0	28.7±0.2

length and temperature of peak brightness and the accuracy of the measurement temperature are listed in Table 1

Experimental procedure

The experiment was performed systematically as follows

After several circular rods of a given pitch had been placed in a flow passage and the flow rate of air had been controlled, an alternating current was supplied to the stainless steel foil heater. The electric current, voltage and room temperature were controlled to set the heated surface temperature in the thermosensitive range of the liquid crystal The bulk temperature of the air at any position between the entrance and the exit was estimated by assuming a linear increase from the entrance to the exit The heat flux, q, was calculated by dividing the net heat flow by the heat transfer area. Thermal conduction effects in the acrylic plate, the stainless steel foil and the cylindrical rod were not taken into account exactly, however, parastic heat losses were evaluated at no flow rate Apparent local heat transfer coefficients and Nusselt numbers were calculated by the following equations

$$\alpha = q/(T_w - T_b) \tag{1}$$

$$Nu = \alpha \cdot D_H/\lambda \tag{2}$$

The scatter of the wall temperature by the present method is within ± 0.4°C as shown in Table 1 The uncertainty of the Nusselt number is within $\pm 15\%$ including a heat flux error of 5% at the lowest Reynolds number $Re = 1000$ It decreases to within $\pm 5\%$ at the highest Reynolds number $Re = 15\,000$ The thermophysical properties appearing in the Nusselt and Reynolds numbers were evaluated at the air temperature Variable properties were not a significant issue since the wall-to-air temperature differences were of the order of 7 C. The Reynolds number is believed to be accurate to $\pm 4\%$

Experiments were carried out for several circular rod pitches, namely $Pi = 57.5$, 46.0, 38.3 and 32.86 mm, and the corresponding ratios of pitch to diameter, Pi/D, are 2.875, 2.3, 1.915 and 1.643, respectively Experimental conditions are listed in Table 2

Table 2 Experimental conditions

Reynolds number	Re	1000 ~ 15000
Heat flux	q (W m^{-2})	115.9 ~ 567.5
Distance between upper and lower plate	H (mm)	10
Pitch of cylindrical rod	Pi (mm)	57.5, 46, 38.3, 32.86
Diameter of cylindrical rod	D (mm)	20

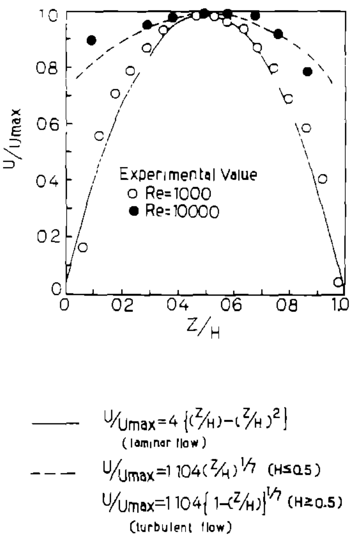

FIG 4 Velocity distribution

The circular rods were set at a longitudinal position of 70 hydraulic diameters from the entrance and also at 19 hydraulic diameters from the starting point of heating. It was recognized that the flow was fully developed and the local heat transfer coefficients approached the thermally developed values for a parallel plate duct with one side heated [1]

Additionally, the velocity distributions across the test section of the water recirculating loop at the measuring station using flow visualization were obtained at $Re = 1000$ and 10 000 in Fig 4 by a laser anemometer These agree with that of the parabolic line for laminar flow and one-seventh law for turbulent flow, respectively Consequently, flow visualization can be related to local heat transfer measurements.

EXPERIMENTAL RESULTS AND DISCUSSION

Temperature distribution

The color distribution of the liquid crystal sheet near several circular rods is shown in Fig. 5 The colors change from blue to yellow, brown and dark brown with decrease of temperature The characteristics of the local heated surface temperatures generated by the interaction of several circular rods can be visualized at a glance Figures 6 and 7 represent isothermal lines Figures 6(a)–(c) show isothermal lines near a circular rod at the center of the width for $Re = 1000$, 4000 and 10 000, and for constant pitch $Pt = 2.3$. For $Re = 1000$, a comparatively high temperature region exists behind each circular rod corresponding to a stagnation region similar to the situation for a single circular rod Isothermal lines associated with a particular rod in a row of rods cease in the downstream region at about $3D$ and move from the center of a rod Interaction effects of circular rods exist between rather than behind rods

Figures 7(a)–(d) show isothermal lines for various pitches at $Re = 2000$ For $Pt/D = 2.875$, the isothermal lines around a circular rod are dumbbell in shape stretching out behind the rod with the rod at the center of one of the knuckles, having high temperature on the outside and colder temperatures on the inside The colder temperature region subdivides into a number of cold islands just behind the rod with one surrounding the rod Symmetrically between rods and about $2D$ downstream there is a high temperature island The dumbbell pattern thins with decreasing Pt/D until at $Pt/D = 1.643$ it has completely changed For $Pt/D = 1.643$, behind the central rod the isothermal lines have a wide closed distribution with three small closed low temperature regions inside, two side by side and one with the rod at the center For the rods either side of the central rod the isothermal lines are contracted These extensions and contractions of isothermal lines appear alternately from rod to rod across the row of rods for comparatively small pitch and depend on the wake flow The accuracy of these isothermal lines is improved on that of a previous publication [1]

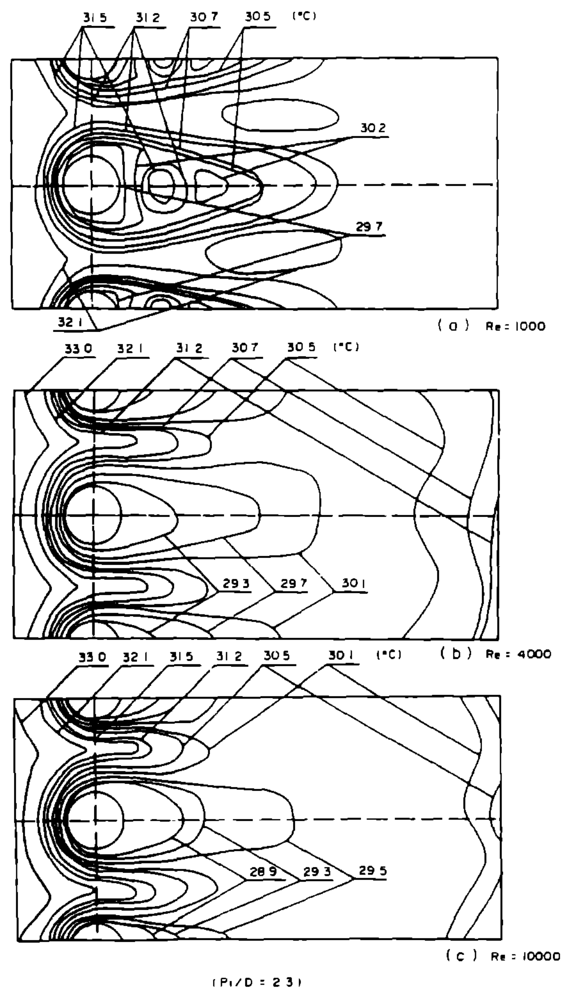

FIG 6. Isothermal maps for various Reynolds numbers ($Pt/D = 2.3$)

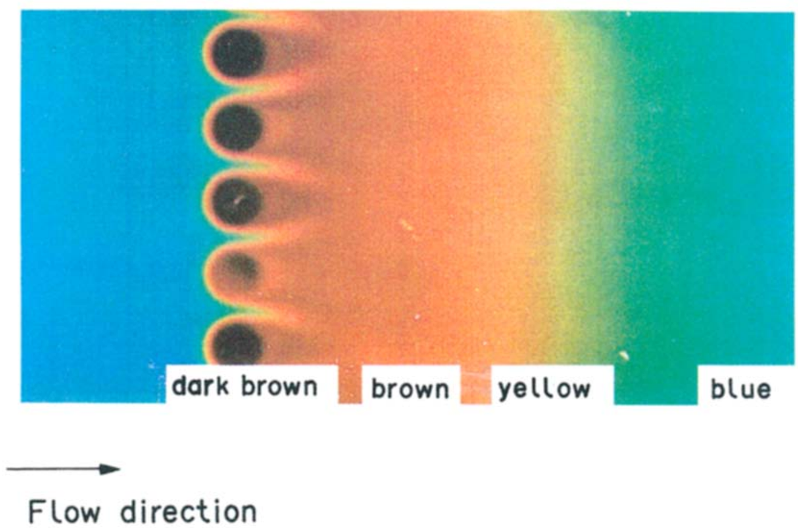

FIG 5 Photograph of the liquid crystal layer showing brightness distribution

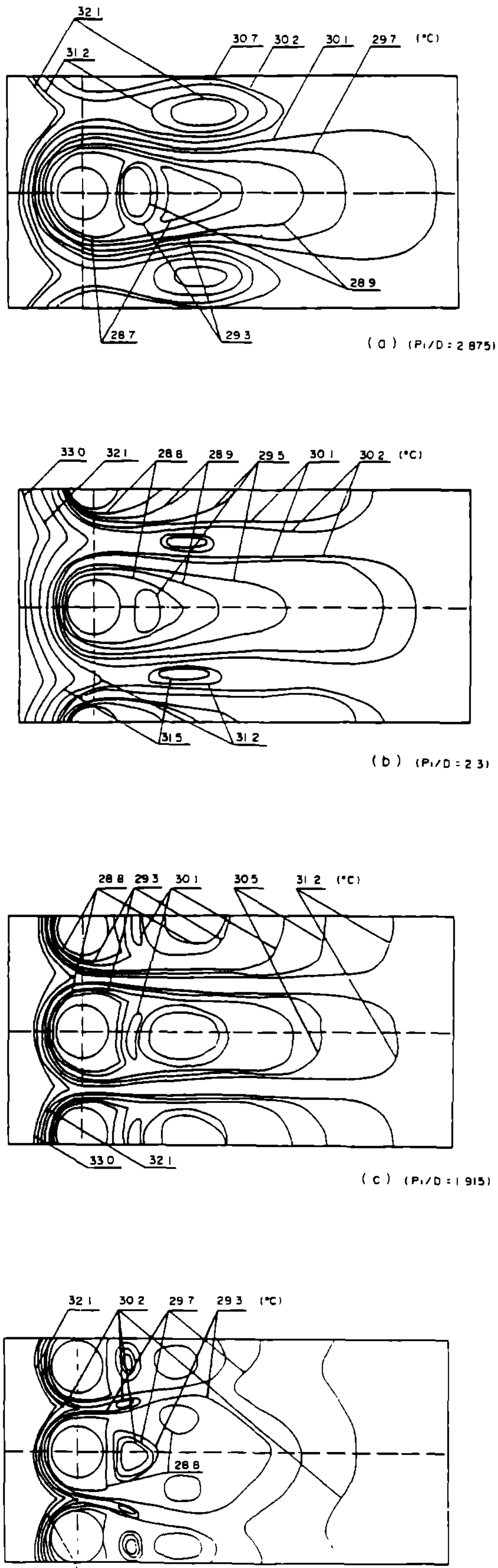

FIG. 7. Isothermal maps for various pitches ($Re = 2000$).

Apparent local Nusselt number

The apparent local Nusselt numbers along the centerline were examined for the longitudinal (x-direction) and the transverse (y-direction) direction.

Figures 8(a) and (b) show longitudinal apparent local Nusselt numbers for various pitches. Figure 8(a) represents the distribution for the upstream direction by expressing X as a negative value from the center of a circular rod. While the effects of pitch on local Nusselt number are insignificant in general for $Pt/D = 1.915$–2.875 for each Reynolds number, the local Nusselt number increases abruptly at $X/D = -0.7$ for $Pt/D = 1.643$. For the downstream case the Nusselt number reaches a minimum just after a rod and then rapidly approaches the fully developed value for $Re = 2000$ (Fig. 8(b)). The position of the minimum value does not depend on pitch. Though less pronounced the minimum does not disappear completely at $Re = 15000$. The effects of pitch are larger in the downstream direction than in the upstream one for a circular rod. Figures 9(a) and (b) show the apparent local Nusselt number as a function of Reynolds number at constant pitch, $Pt/D = 2.3$. The longitudinal gradient of local Nusselt number becomes greater with increase of Reynolds number for the upstream case (Fig. 9(a)). In Fig. 9(b), the Nusselt number becomes minimal at $X/D = 1.25$ for $Re = 1000$ and at $X/D = 1.0$ for $Re = 2000$. The position tends to approach the circular rod with increase of Re. These kinds of minimum values do not appear at Reynolds numbers larger than $Re = 2000$, within the present accuracy.

Figures 10(a) and (b) show the apparent local Nusselt number between two circular rods for various pitches (Fig. 10(a)) and Reynolds numbers (Fig. 10(b)). In Fig. 10(a), the local Nusselt number has a minimum value midway between two circular rods and the distribution is symmetrical about the minimum position. These minimum values increase with decrease of pitch and the present tendency does not depend on Reynolds number qualitatively. In Fig. 10(b), the effects of Reynolds number on the magnitude of Nusselt number are shown.

From the experimental data an attempt has been made to obtain an empirical equation for apparent local Nusselt number between two circular rods. Figure 11 shows representatively the relationship between Nu and y/D from the side surface of a circular rod to midpitch between two rods in logarithmic form. According to this figure, the relationship between Re, y/D and Nu can be expressed by the following function $Nu \sim Re^{m}(y/D)^{n}$. The index of y/D, n, is a function of Re and Pt/D and is represented as a parameter of Pt/D in Fig. 12. The value is shown in absolute form in the figure since n is negative. The absolute value of n changes with $Re^{0.220}$. The index n is expressed in the following equation

$$n = -0.223 Re^{0.220} (Pt/D)^{-0.712} \quad (3)$$

The index m depends on Re but not continuously. It

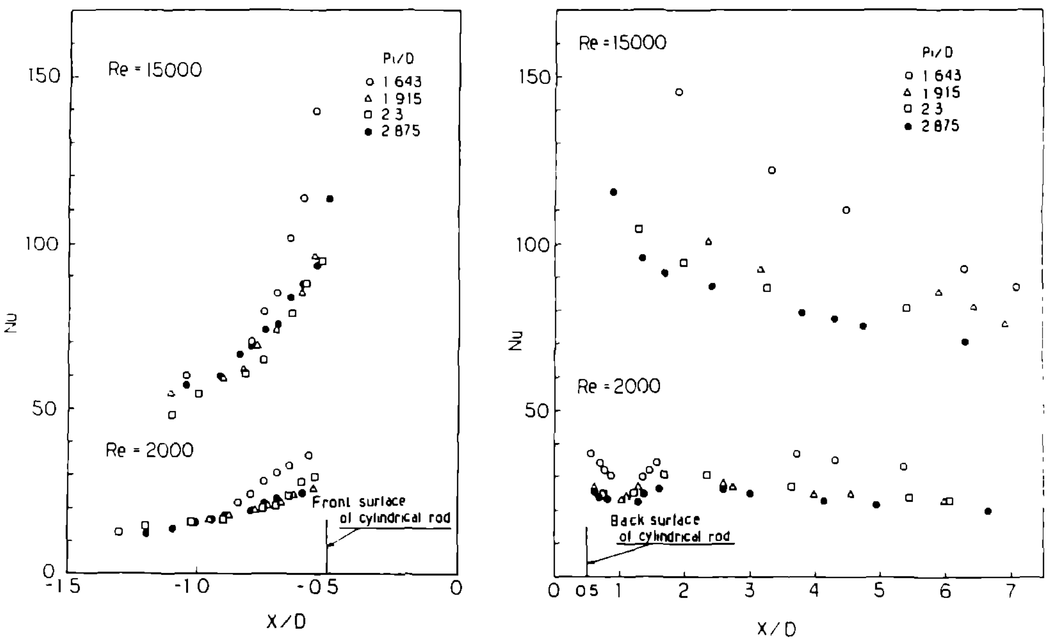

(a) Upstream (b) Downstream

Fig. 8. Longitudinal distribution of local Nusselt number for various pitches.

has been found that the apparent local Nusselt number between two circular rods can be represented by the following equations

for $Re < 2000$,

$$Nu = 0.979Re^{0.372}(y/D)^n \quad (4)$$

for $Re > 2000$,

$$Nu = 0.236Re^{0.569}(y/D)^n \quad (5)$$

where n is expressed in equation (3). These equations agree with experimental values within $\pm 15\%$.

Flow visualization

In order to relate heat transfer to flow, flow visualization experiments were performed.

Figures 13(a) and (b) show steady flow for $Re = 1000$, 2000 and 6000 at $Pi/D = 2.875$. Figure 13(a) shows photographs of the main flow taken by

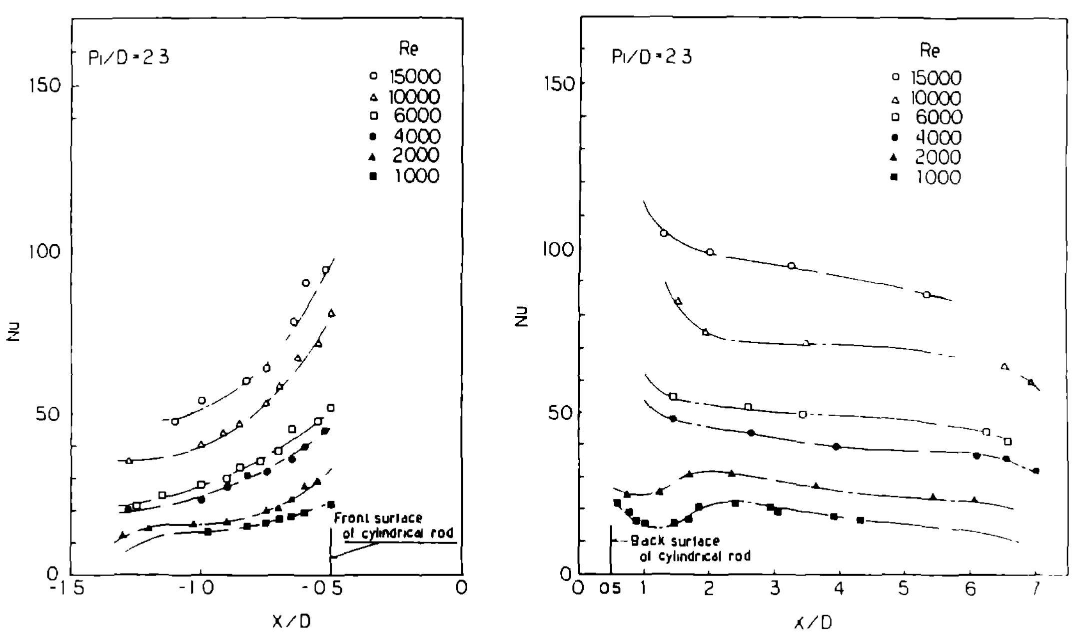

(a) Upstream (b) Downstream

Fig. 9. Longitudinal distribution of local Nusselt number for various Reynolds numbers.

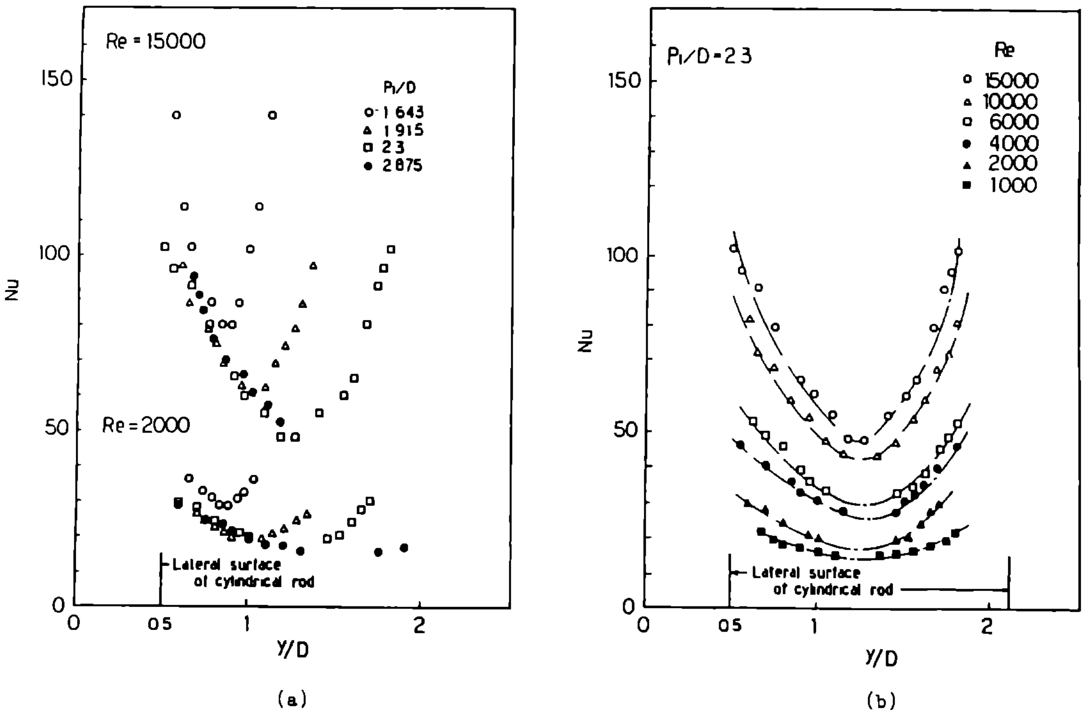

Fig 10. Local Nusselt number between two circular rods

illuminating the longitudinal slit light in the vertical direction across the section at midspan position The main flow separates from the circular rods in the downstream direction and separation regions occur on each rod surface Figure 13(b) shows the patterns with pearl pigments laid on the lower plate. These flow patterns are independent for each circular rod and correspond to the local heat transfer. This is called the steady and independent case (domain A in Fig 16). Figure 14 shows the flow characteristics for $Re = 1000$ and 2000 at $Pi/D = 1.915$. Near the rear facing surface of the circular rods, the flow pattern is composed of extended or contracted wakes by interference of circular rods and does not change with time. This is called steady and interfering situation (domain B in Fig. 16).

For $Pi/D = 1.915$ and $Re > 3000$ the flow patterns were not clear and so light was illuminated from a tangential direction on the lower plate to get better results. Figure 15 shows photographs at various times. These figures represent the flow patterns that change with time because of unstable interference. This is called the unsteady and interfering case (domain C in Fig 16).

Figure 16 shows the correspondence between heat transfer and flow The ordinate is Re and abscissa Pi/D. Three kinds of symbols represent temperature regions which are independent, slight interferential or interferential Signs A, B and C represent the domains

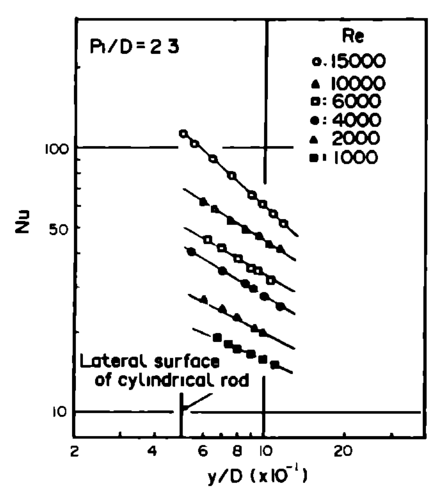

Fig. 11. Logarithmic relationship between Nu and y/D

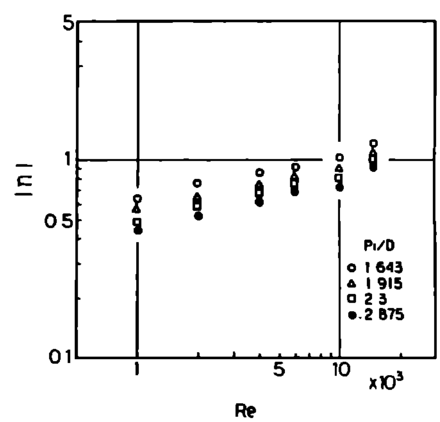

Fig 12 Index of y/D

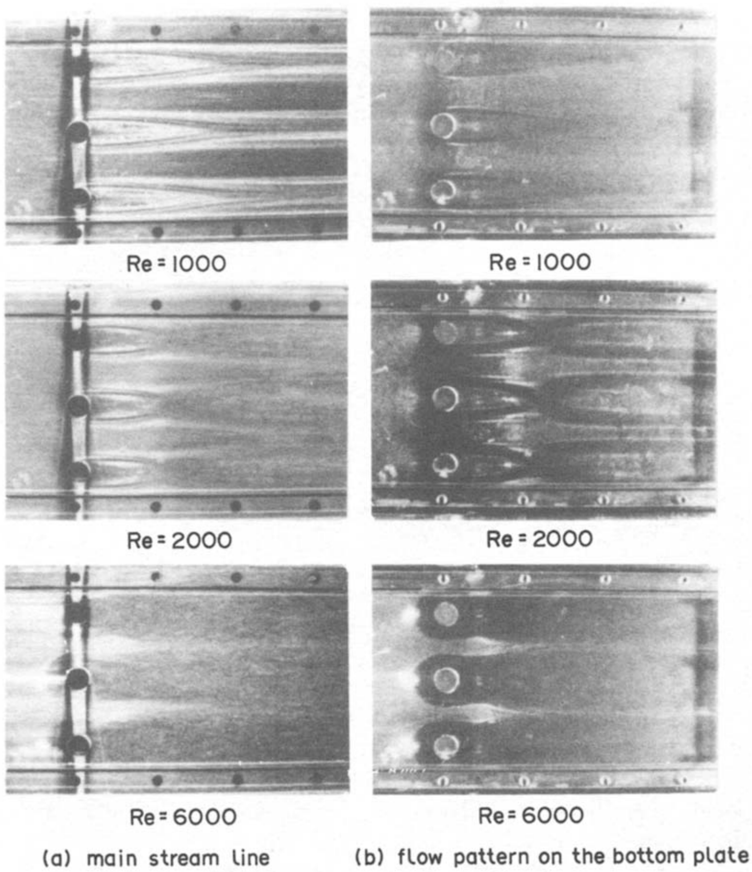

FIG. 13. Steady and regular flow patterns ($Pt/D = 2.875$): (a) main stream line; (b) flow pattern on the bottom plate ($Pt/D = 1.915$).

described above, and solid lines show their boundaries. The dashed domain expresses the flow visualized region. These situations of heat transfer and flow patterns agree with each other. However, the complicated mechanism should be studied in detail in the future.

CONCLUDING REMARKS

The effects of a single row of spaced circular rods were studied on heat transfer and flow in a parallel plate duct.

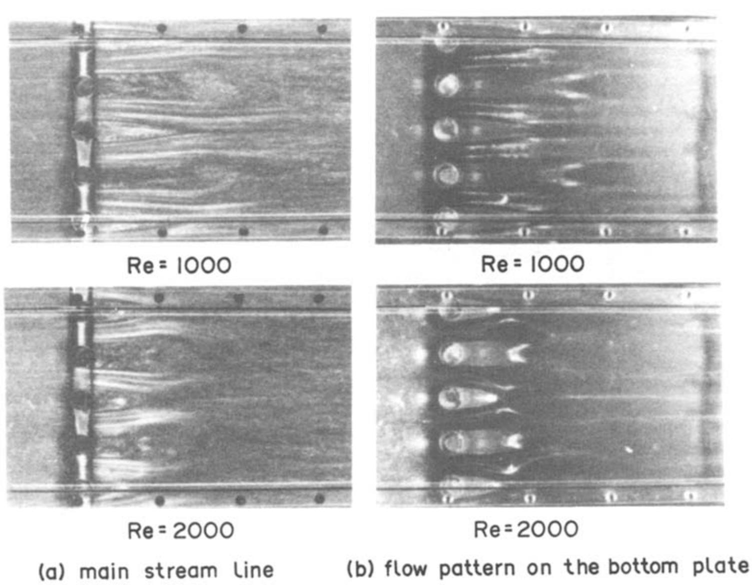

FIG. 14. Steady and irregular flow patterns: (a) main stream line; (b) flow pattern on the bottom plate.

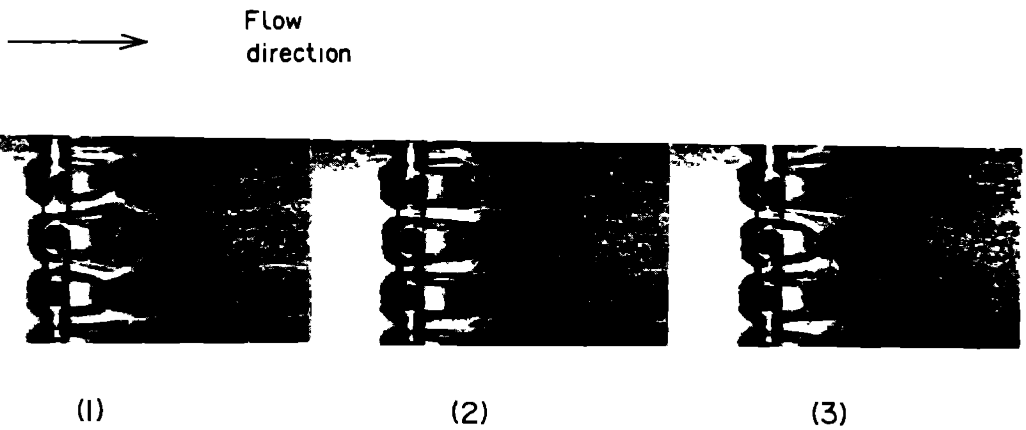

FIG. 15 Unsteady and irregular pattern ($Pi/D = 1.915$, $Re = 3000$)

(1) A thermosensitive liquid crystal sheet was used to measure temperature distributions. A method based on optical filters with sharp-band-pass characteristics was applied so that human color perception could be avoided. This method was shown to be useful even under high temperature gradients.

(2) Apparent local Nusselt numbers between two circular rods were expressed by a power relationship of Reynolds number Re and dimensionless distance y/D The index for y/D is a function of Re and dimensionless pitch Pi/D.

(3) For comparatively large pitch, heat transfer and flow characteristics were similar to the pattern in the case of a single rod. On the other hand, for small pitch the flows around circular rods interact with each other, and the wake flow region and isothermal lines extend or contract behind circular rods Flow characteristics behind circular rods are divided into three regions depending on the values of Reynolds number and pitches of rods

Acknowledgements—We would like to thank Professor H Kawamura, Science University of Tokyo and Dr M Hishida,

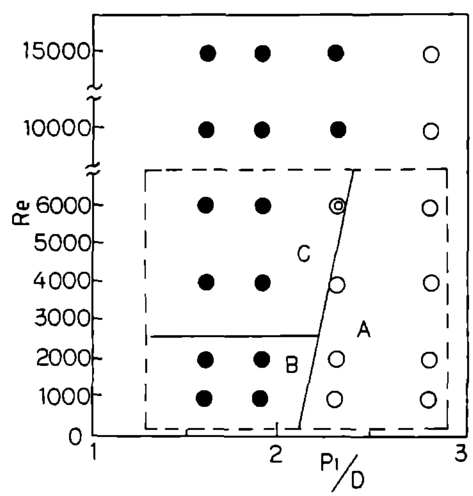

- - - - - Flow visualized region

Regime	Flow Pattern
A	Steady and Regular Pattern
B	Steady and Irregular Pattern
C	Unsteady and Irregular Pattern

Symbol	Temperature Distribution
○	Even and Independent Distribution
◎	Slightly Uneven and Interferential Distribution
●	Uneven and Interferential Distribution

FIG 16. Correspondence between heat transfer and flow pattern

Japan Atomic Research Institute, who advised us to undertake the present study, and Mr K Mitsushiro, Matsushita Electronic Ltd , who helped with our experiments

REFERENCES

1 K Ichimiya, N Akino, T Kunugi and K Mitsushiro, Fundamental study of the heat transfer and flow situation around a spacer (in the case of a cylindrical rod as a spacer), *Int. J Heat Mass Transfer* **31**, 2215–2225 (1988)

2 J Ward and M A Jewad, Local and heat transfer associated with a single row of closely-spaced tubes in cross flow, *Proc 6th Int Heat Transfer Conf*, Toronto Vol 4, pp 273–278 (1978).

3 S Aiba, H Tsuchida and S Umeshima, Heat transfer of single rows in cross flow of air, *Proc 19th Japan Natn Heat Transfer Symp*, Vol 1, pp 88–90 (1982)

4 M Kumada, M Hiwada, M Itoh and I Mabuchi, Heat transfer on three circular tubes normal to a stream, *Proc 19th Japan Natn Heat Transfer Symp*, Vol. 1, pp 91–93 (1982)

5 O L. Pierson, Experimental investigation of the influence of tube arrangement on convection heat transfer and flow resistance in cross flow of gases over tube banks, *Trans ASME* **59**, 563–572 (1937).

6 E D Grimison, Correlation and utilization of new data on flow resistance and heat transfer for crossflow of gases over tube banks, *Trans ASME* **59**, 583–594 (1937)

7 O P Bergelin, E S Davis and H L Hull, A study of three tube arrangements in unbaffled tubular heat exchangers, *Trans ASME* **71**, 369–374 (1949)

8 E C Huge, Experimental investigation of effects of equipment size on convection heat transfer and flow resistance in cross flow of gases over tube banks, *Trans ASME* **59**, 573–581 (1937)

9 G J VanFossen, Heat transfer coefficients for staggered arrays of short pin fins, ASME Paper 81-GT-75, pp 1–11 (1981)

10 C den Ouden and C J Hoogendorn, Local convective heat transfer coefficients for jets impinging on a plate, experiments using a liquid-crystal technique, *Proc 5th Int Heat Transfer Conf*, Tokyo, Vol 5, pp 293–297 (1974)

11 T E. Cooper, R J Field and J F Meyer, Liquid crystal thermography and its application to the study of convective heat transfer, *Trans ASME*, Ser C **97**, 442–450 (1975)

12 P T Ireland and T V Jones, Detailed measurements of heat transfer on and around a pedestal in fully developed passage flow, *Proc 8th Int Heat Transfer Conf*, San Francisco, Vol 3, pp 975–980 (1986)

13 S A Hippensteele, L M Russel and F J Torres, Use of a liquid-crystal, heater-element composite for quantitative, high-resolution heat transfer coefficients on a turbine airfoil, including turbulence and surface roughness effects, NASA Technical Memorandum 87355, pp 1–13 (1987)

14 N Akino, T Kunugi, K Ichimiya, K Mitsushiro and M Ueda, Improved liquid-crystal thermometry excluding human color sensation, *Trans ASME*, Ser C **111**, 558–565 (1989)

UNE ETUDE FONDAMENTALE DU TRANSFERT THERMIQUE ET DE L'ECOULEMENT AUTOUR DES ESPACEURS (UNE SEULE NAPPE DE PLUSIEURS CYLINDRES EN ATTAQUE FRONTALE)

Résumé—On décrit les caractéristiques du transfert thermique et de l'écoulement autour de plusieurs espaceurs (une seule nappe de plusieurs cylindres) en attaque frontale sur une surface chaude dans un conduit à plan parallèle. Les distributions de température sont obtenues en utilisant un film thermosensible à cristal liquide et une méthode de filtre optique à bande étroite qui ne nécessite pas la perception humaine des couleurs Le nombre de Nusselt local apparent entre deux cylindres est exprimé en fonction du nombre de Reynolds, de la localisation et du pas des cylindres. Le pas et le nombre de Reynolds affectent les configurations de l'écoulement en sillage qui sont classées en trois domaines

EINE GRUNDLEGENDE UNTERSUCHUNG VON WARMEÜBERGANG UND STRÖMUNG IN DER UMGEBUNG VON ABSTANDSHALTERN (EINE EINZELNE REIHE VON ZYLINDRISCHEN, QUER ANGESTRÖMTEN STIFTEN)

Zusammenfassung—In dieser Arbeit werden Warmeubergang und Stromung in der Umgebung einiger Abstandshalter untersucht, die durch eine einzelne Reihe von zylindrischen Stiften bestehen Diese befinden sich zwischen parallelen Platten, von denen eine beheizt ist, und werden quer angestromt. Unter Verwendung eines temperaturempfindlichen Films aus Flussigkristallen wird die Temperaturverteilung ermittelt Die Verwendung eines optischen Schmalbandfilters ermoglicht es, daß die Auswertung nicht auf das menschliche Farbempfinden angewiesen ist Die scheinbaren ortlichen Nusselt-Zahlen zwischen zwei zylindrischen Stiften werden in Abhängigkeit der Reynolds-Zahl, der Position und des Abstandes zwischen den Zylindern ausgedruckt Abstand und Reynolds-Zahl beeinflussen die Formen des Nachlaufs, die in drei Bereiche eingeteilt werden

ФУНДАМЕНТАЛЬНОЕ ИССЛЕДОВАНИЕ ТЕПЛОПЕРЕНОСА И ОБТЕКАНИЯ ПРОСТАВОК (ПОПЕРЕЧНОЕ ОБТЕКАНИЕ ЕДИНИЧНОГО РЯДА ИЗ НЕСКОЛЬКИХ ЦИЛИНДРИЧЕСКИХ СТЕРЖНЕЙ)

Аннотация—Описываются характеристики теплопереноса и обтекания нескольких проставок (поперечно обтекаемый единичный ряд из нескольких цилиндрических стержней) в плоскопараллельном канале Распределения температур получени с использованием термочувствительной пленки из жидких кристаллов при помощи узкополосных оптических фильтров, что позволяет отказаться от определения цвета человеком. Локальные значения числа Нуссельта в области между двумя цилиндрическими стержнями выражены как функция числа Рейнольдса, расположения цилиндрических стержней и шага между ними. Как шаг, так и число Рейнольдса оказывают влияние на картину течения в следе, где можно выделить три области.